Contract No:

This document was prepared in conjunction with work accomplished under Contract No. DE-AC09-08SR22470 with the U.S. Department of Energy (DOE) Office of Environmental Management (EM).

Disclaimer:

1 EVALUATION OF CERAMIC WASTE FORMS – COMPARISON OF HOT ISOSTATIC PRESSED AND MELT PROCESSED FABRICATION METHODS

Savannah River National Laboratory (SRNL) is developing melt-processed reference ceramic waste forms for treatment of waste streams generated by reprocessing commercial used nuclear fuel. The waste form is designed to crystallize into an engineered multiphase ceramic upon cooling from a melt (i.e. melt processing). Compositions are designed based on combinations of the waste and additives to target various phases. Elements with a +3 or +2 valance form perovskite ($(A^{+2})TiO_3$) and pyrochlore ($(A^{+3})_2Ti_2O_7$) type phases.[1,2] Zirconium (+4 valence) partitions to a zirconolite ($CaZrTi_2O_7$) phase.[3] Cs and Rb elements partition to a hollandite structure based on the general formula $Ba_xCs_yM_zTi^{+4}_{8-z}O_{16}$ where z = 2x+y for trivalent cations and z = x+y/2 for divalent cations for charge compensation.[4-6] The targeted phase assemblage utilized at SRNL is based on the synthetic rock (SYNROC) family of titanate ceramics, the design of which is built on the concept of simulating naturally occurring minerals that have immobilized radionuclides over geologic timescales.[7,8] While the majority of SYNROC compositions are produced via hot isostatic pressing (HIP), earlier work conducted at SRNL has demonstrated that these materials can be successfully fabricated by melt processing under appropriate conditions.[9-12]

FY16 efforts were focused on direct comparison of multi-phase ceramic waste forms produced via melt processing and HIP methods. Based on promising waste form compositions previously devised at SRNL[13], simulant material was prepared at SRNL and a portion was sent to the Australian Nuclear Science and Technology Organization (ANSTO) for HIP treatments, while the remainder of the material was melt processed at SRNL. The microstructure, phase formation, elemental speciation, and leach behavior, and radiation stability of the fabricated ceramics was performed. In addition, melt-processed ceramics designed with different fractions of hollandite, zirconolite, perovskite, and pyrochlore phases were investigated. for performance and properties. Table 1 lists the samples studied.

Table 1. Multi-phase waste form baseline compositions fabricated via melt processing and HIP.

Designation	Hollandite (wt. %)	Zirconolite (wt. %)	Pyrochlore (wt. %)	Perovskite (wt. %)	Metal (wt. %)	Fabrication Method
HIP-1250*	65.4	14.61	16.84	2.54	0.61	HIP: 1250 °C
HIP-1300*	65.4	14.61	16.84	2.54	0.61	HIP: 1300 °C
CAF-11113*	65.4	14.61	16.84	2.54	0.61	Melt Processing
CAF-21113	48.59	21.71	25.02	3.78	0.9	Melt Processing
CAF-41113	32.09	28.68	33.05	4.99	1.19	Melt Processing
CAF-21223	57.06	25.5	14.69	2.22	0.53	Melt Processing
CAF-22123	55.67	12.51	28.83	2.18	0.52	Melt Processing

*Baseline composition

Representative scanning electron microscopy (SEM) and energy dispersive spectroscopy (EDS) analysis of the as fabricated HIPed and melt-processed samples are presented in Figure 1 and Figure 2. Significant differences in the grain microstructure, the phase assemblage, and the elemental speciation were evident.

The melt-processed samples exhibited characteristic large hollandite grains (darker gray areas) surrounded by zirconolite, pyrochlore, and perovskite phases (lighter gray areas). Very small regions with an almost black hue were found to consist primarily of TiO_2. The Ba, Ti, Cr, Fe, and Al (not shown) elemental maps clearly indicate the formation of large hollandite grains. However, higher concentrations of Cr were observed at the interior of many hollandite grains, while Al (not shown) and Fe were found in

higher concentrations near the grain boundaries. Upon cooling from a melt, it is possible that Cr-rich regions crystallize into the hollandite phase first due to the higher melting point of Cr_2O_3. Ideally, a significant portion of the Cs remaining in the system will be immobilized at this point. The remaining liquid in the system is then deficient in Cr and, upon cooling to a suitably low temperature, the crystallization of hollandite rich in Al and Fe occurs.

Another notable feature of the melt-processed samples is the close correspondence among Ca, Zr, and Nd in the elemental maps. In the zirconolite structure, Ca^{2+} or Zr^{4+} can be substituted by Nd^{3+}, and extensive Nd substitution into the zirconolite structure leads to partitioning into pyrochlore and/or perovskite phases. [9,10] While more precise determinations of compound stoichiometries in the Ca-Nd-Zr areas of the melt-processed samples are on-going, it is likely that nominal compositions of $Ca_{1-x}Zr_{1-x}Nd_{2x}Ti_2O_7$ are forming and partitioning into various doped perovskite and pyrochlore phases occurs at critical Nd concentrations.

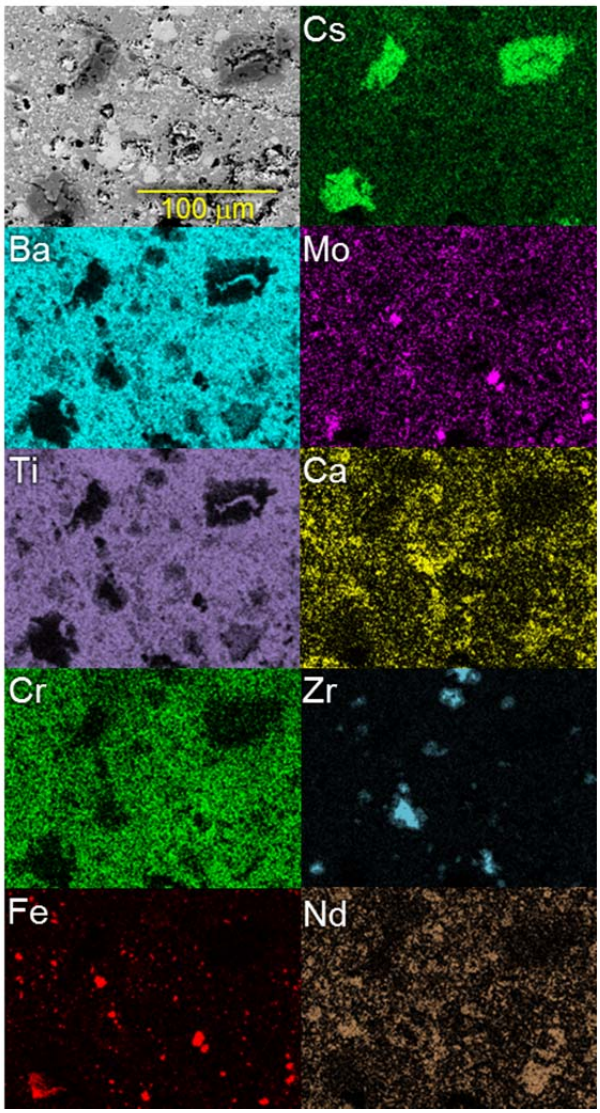

Figure 1. SEM image and corresponding elemental maps of a sample HIPed at 1300°C

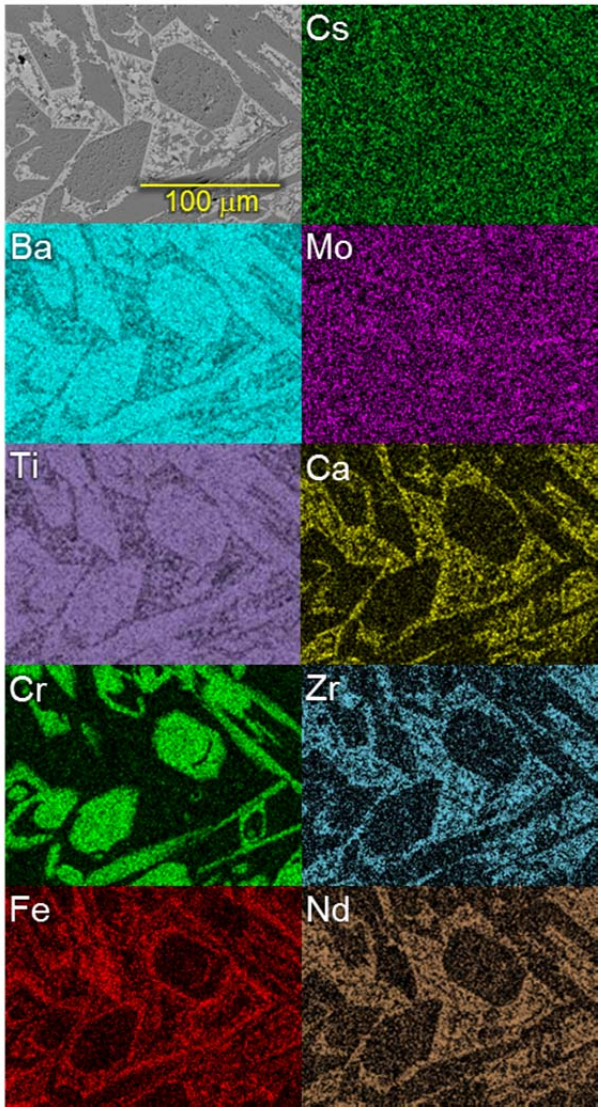

Figure 2. SEM image and corresponding elemental maps of a CAF-11113 sample melt processed at 1625°C

The HIPed samples exhibited a more fine-grained microstructure characteristic of a solid-state densification process and displayed significant microstructural differences compared to the melt-processed samples. The HIPed samples exhibited raised "islands" rich in Cs (dark in color in the SEM image) and appeared to be a Cs-titanate phase. This phase is consistent with the results of earlier work, where it was suggested that partial melting at HIP temperatures of 1300 – 1350 °C results in Cs partitioning between the hollandite phase and an intergranular melt phase.[14] There was a correspondence between the Fe and Mo maps at several locations across the sample, suggesting the formation of a Fe-Mo compound. Also of significance is the speciation of Ca, Nd, and Zr compared to the the melt-processed samples. In the melt-processed specimens, many regions were found to contain Ca, Nd, and Zr in comparable concentrations. In the HIPed samples, higher concentrations of Zr were found in localized regions suggesting that the regions of high Zr content could be ZrO_2 or $ZrTiO_4$ along with a doped perovskite phase.

Transmission electron microscopy (TEM) with Energy-dispersive X-ray spectroscopy (EDX) was used to further identify crystalline phases and chemical composition in the multiphase ceramic waste form samples. Based on selected area electron diffraction (SAED) patterns and EDX spectra, a hollandite phase (Ba, Al, Cr, Fe, Ti, O), zirconolite/pyrochlore phases (Ca, Zr, Nd, Ti, O), and a perovskite phase (Sr, Ca, Ti, O) were identified in the melt-processed baseline sample. In the HIPed sample, major crystalline phases including hollandite and zirconolite were found in addition to a phase not observed in the melt-processed sample and with chemical species including Ti, Cr, Fe, Mo, and O. Additionally, a perovskite phase was not observed in the HIPed sample. Figure 3 shows a high resolution TEM observation of an interface between hollandite and zirconolite phases in the baseline melt-processed sample.

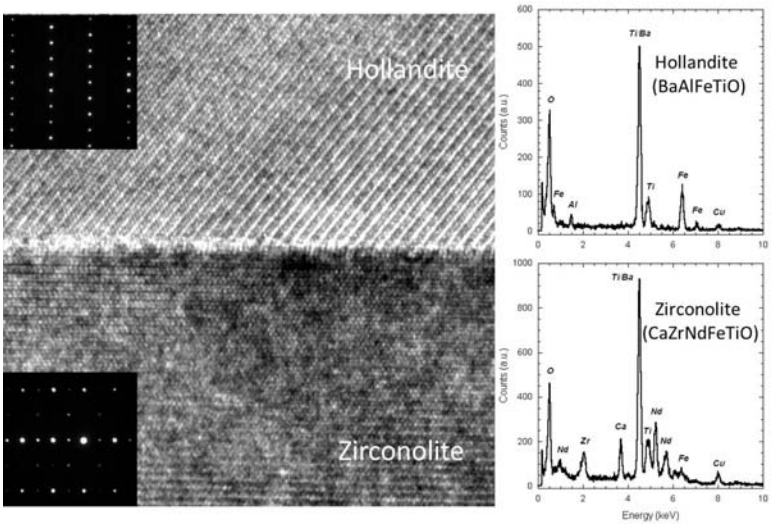

Figure 3. High resolution TEM observation of interface between hollandite and zirconolite phases in CAF-11113, including corresponding SAED patterns and EDX spectrums.

Monolith leach tests were performed over 28 days to assess the chemical durability of melt-processed and HIPed samples. Shown in Figure 4 is the Cs fractional release for the melt processed and HIPed baseline composition as well as several other melt-processed compositions with varying targeted phase assemblages. It is evident that the Cs retention characteristics of the melt-processed baseline sample were superior to those of the other compositions. Although the sample HIPed at 1250°C exhibited less Cs release compared to the sample HIPed at 1300°C, both exhibited greater Cs release compared to melt-processed sample of the same composition. Although the initial leach data provided are encouraging, it should be noted that the leach test data for other waste elements, including Mo and Sr, are still being analyzed.

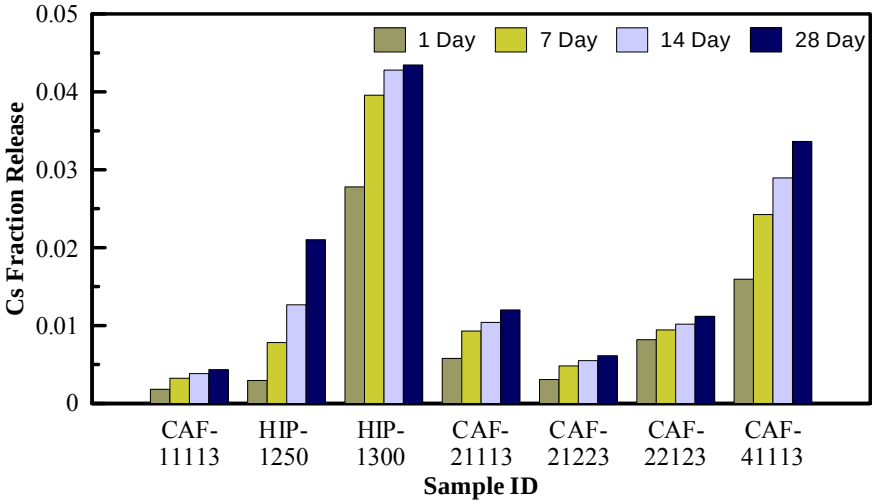

Figure 4. Fractional release of Cs from melt-processed and HIPed waste forms.

Melt-processed and HIPed samples were also irradiated with 400 keV Kr ions at a fluence of 5×10^{14} ions/cm^2, corresponding to a dose level ~1 displacement per atom (dpa). Radiation-induced microstructural evolution was investigated by cross-sectional TEM observation. The present study was focused on the hollandite and zirconolite phases. The TEM results, shown in Figure 5, indicate that the melt-processed and HIPed samples experience an nearly identical (even thickness of damage layer) amorphous transformation from crystalline under ion irradiation suggesting that fabrication method does not affect radiation stability of the crystalline phases.

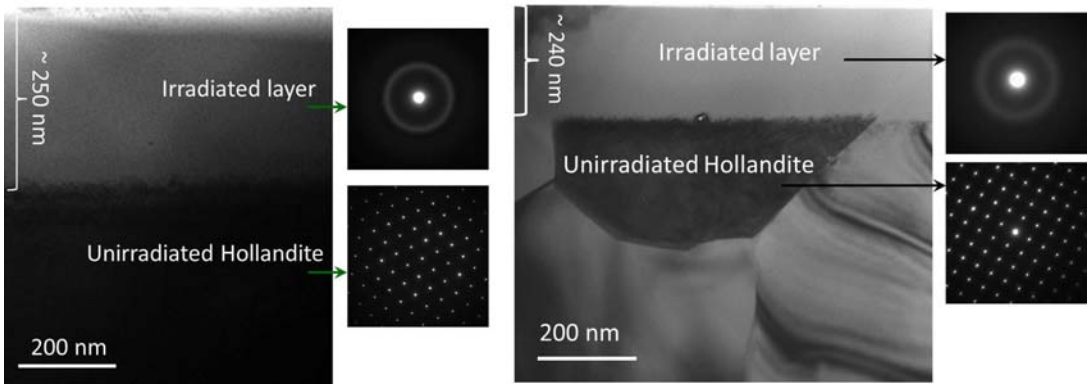

Figure 5. TEM observation of hollandite phase in irradiated CAF-11113 (left) and SW-1732 (right) samples.

2 SYNERGISTIC ACTIVITIES

A Cooperative Research and Development Agreement (CRADA) with ANSTO has also been in place to support the project. As part of the CRADA, the compositions developed at SRNL were prepared (HIPed) at ANSTO and subsequently characterized by ANSTO, SRNL, and LANL. In addition, this work package is augmented by DOE-NEUP projects that are being conducted collaboratively with Alfred University (AU) and Clemson University. SRNL performed chemical leach testing and analysis on various "designer" ceramic waste form materials being explored as a strategy to optimize the ceramic waste form through tailoring the amount and composition of the crystalline phases in the final waste form. Additionally, a student from Clemson University worked at SRNL during the summer to prepare, test, and analyze Ga-doped ceramic waste forms. Preliminary results indicate the retention of certain mobile species in aqueous environments can be significantly affected by the stoichiometry of the primary phases.

3 LIST OF PUBLICATIONS

J. W. Amoroso, J. Marra, C. S. Dandeneau, K. Brinkman, Y. Xu, M. Tang, V. Maio, S. Webb and W. K. S. Chiu, "Cold Crucible Induction Melter Test for Crystalline Ceramic Waste Form Fabrication: A Feasibility Assessment," J. Nucl. Mater., pp. (submitted).

M. Tang, P. Tumurugoti, B. M. Clark, S. K. Sundaram, J. Amoroso, J. Marra, C. Sun, P. Lu, Y. Wang and Y.-B. Jiang, "Heavy ion irradiations on synthetic hollandite-type materials: $Ba_{1.0}Cs_{0.3}A_{2.3}Ti_{5.7}O_{16}$ (A = Cr, Fe, Al)," J. Solid State Chem., 239 pp. 58-63, (2016).

4 SYNERGISTIC PUBLICATIONS

A. P. Cocco, M. B. DeGostin, J. A. Wrubel, P. J. Damian, T. Hong, Y. Xu, Y. Lin, P. Pianetta, J. Amoroso, K. S. Brinkman and W. K. S. Chiu, "Three-Dimensional Mapping of Crystalline Ceramic Waste Form Materials," J. Am. Ceram. Soc., pp. (submitted).

B. M. Clark, P. Tumurugoti, S. K. Sundaram, J. Amoroso, J. Marra, V. Shutthanandan and M. Tang, "Radiation Damage of Hollandite in Multiphase Ceramic Waste Forms," Nucl. Instrum. Methods Phys. Res., Sect. B, pp. (submitted).

Y. Xu, Y. Wen, R. Grote, J. Amoroso, L. Shuller Nickles and K. S. Brinkman, "A-site compositional effects in Ga-doped hollandite materials of the form $Ba_xCs_yGa_{2x+y}Ti_{8-2x-y}O_{16}$: implications for Cs immobilization in crystalline ceramic waste forms," Sci. Rep., 6 pp. 27412, (2016).

P. Tumurugoti, S. K. Sundaram, S. T. Misture, J. C. Marra and J. W. Amoroso, "Crystallization behavior during melt-processing of ceramic waste forms," J. Nucl. Mater., 473 pp. 178-188, (2016).

F. Rabbi, K. Brinkman, J. Amoroso and K. Reifsnider, "Finite Element analysis of ion transport in Solid State Nuclear Waste Form Materials," Comput. Mater. Sci., pp. (submitted).

J. Wen, C. Sun, P.P. Dholabhai, Y. Xia, M. Tang, D. Chen, D.Y. Yang, Y.H. Li, B.P. Uberuaga, Y.Q. Wang, “Temperature dependence of the radiation tolerance of nanocrystalline pyrochlores A2Ti2O7 (A: Gd, Ho and Lu)”, Acta Mater., 110 (2016) 175-184.

Ming Tang, James A. Valdez, Yongqiang Wang, Jian Zhang, Blas P. Uberuaga, Kurt E. Sickafus, “Ion irradiation-induced crystal structure changes in inverse spinel MgIn2O4”, Scripta Mater., 125 (2016) 10–14.

Blas Pedro Uberuaga, Ming Tang, Chao Jiang, James A. Valdez, Roger Smith, Yongqiang Wang & Kurt E. Sickafus, “Opposite correlations between cation disordering and amorphization resistance in spinels versus pyrochlores”, Nature Comms, 9750 (2015).

Ming Tang, Andrew T. Nelson, Elizabeth S.Wood, Stuart A. Maloy, Ying-Bing Jiang, “Grazing incidence X-ray diffraction and transmission electron microscopy studies on the oxide formation of molybdenum in a water vapor environment”, Scripta Mater., 120 (2016) 49–53.

5 REFERENCES

1. D. S. D. Gunn, N. L. Allan, H. Foxhall, J. H. Harding, J. A. Purton, W. Smith, M. J. Stein, I. T. Todorov and K. P. Travis, "Novel Potentials for Modelling Defect Formation and Oxygen Vacancy Migration in $Gd_2Ti_2O_7$ and $Gd_2Zr_2O_7$ Pyrochlores," *J. Mater. Chem.*, **22** [11] pp. 4675-4680, (2012).

2. R. Ubic, I. M. Reaney and W. E. Lee, "Perovskite $NdTiO_3$ in Sr- and Ca-doped $BaO-Nd_2O_3-TiO_2$ Microwave Dielectric Ceramics," *J. Mater. Res.*, **14** [04] pp. 1576-1580, (1999).

3. H. F. Xu and Y. F. Wang, "Crystallization Sequence and Microstructure Evolution of Synroc Samples Crystallized from $CaZrTi_2O_7$ Melts," *J. Nucl. Mater.*, **279** [1] pp. 100-106, (2000).

4. V. Aubin-Chevaldonnet, D. Caurant, A. Dannoux, D. Gourier, T. Charpentier, L. Mazerolles and T. Advocat, "Preparation and Characterization of $(Ba,Cs)(M,Ti)_8O_{16}$ ($M = Al^{3+}$, Fe^{3+}, Ga^{3+}, Cr^{3+}, Sc^{3+}, Mg^{2+}) Hollandite Ceramics Developed for Radioactive Cesium Immmobilization," *J. Nucl. Mater.*, **366** [1-2] pp. 137-160, (2007).

5. M. L. Carter, E. R. Vance, D. R. G. Mitchell and Z. Zhang, "Mn Oxidation States in $Ba_xCs_yMn_zTi_{8-z}O_{16}$," *Mat. Res. Soc. Symp. Proc.*, **824** pp. CC4.6.1 - 6, (2004).

6. M. L. Carter, E. R. Vance and H. Li, "Hollandite-rich Ceramic Melts for Immobilization of Cs," *Mat. Res. Soc. Symp. Proc.*, **807** pp. 249-254, (2003).

7. I. W. Donald, "Immobilization of Radioactive materials as a Ceramic Wasteform," pp. 185-203 in Vol. *Waste Immobilization in Glass and Ceramic Based Hosts: Radioactive, Toxic and Hazardous Wastes*. Edited by John Wiley & Sons, Great Britain,2010.

8. A. E. Ringwood, S. E. Kesson, N. G. Ware, W. Hibberson and A. Major, "Immobilization of High-level Nuclear-Reactor Wastes in SYNROC," *Nature*, **278** [5701] pp. 219-223, (1979).

9. J. Amoroso, J. Marra, S. D. Conradson, M. Tang and K. Brinkman, "Melt Processed Single Phase Hollandite Waste Forms for Nuclear Waste Immobilization: Ba1.0Cs0.3A2.3Ti5.7O16; A = Cr, Fe, Al," *J. Alloy Compd.*, **584** pp. 590-99, (2014).

10. J. Amoroso, J. C. Marra, M. Tang, Y. Lin, F. Chen, D. Su and K. S. Brinkman, "Melt processed multiphase ceramic waste forms for nuclear waste immobilization," *J. Nucl. Mater.*, **454** [1-3] pp. 12-21, (2014).

11. J. W. Amoroso, "Material Recovery & Waste Form Development – Ceramics Formulation optimization activities in FY15 – Preliminary Results (M4FT-15SR0307025)," *US Department of Energy Report SRNL-L3100-2015-00185, Internal Memorandum,* Savannah River National Laboratory, Aiken SC (2015).

12. K. Brinkman, J. Amoroso, J. Marra and M. Tang, "Crystalline Ceramic Waste Forms: Comparison of Reference Process for Ceramic Waste Form Fabrication," *US Department of Energy Report SRNL-STI-2013-00442 (FCRD-SWF-2013-000229),* Savannah River National Laboratory, Aiken SC (2013).

13. J. W. Amoroso and J. C. Marra, "Melt Processed Crystalline Ceramic Waste Forms for Advanced Nuclear Fuel Cycles - Final CRP Report for Research Agreement No. 17208," *US Department of Energy Report SRNL-STI-2015-00437,* Savannah River National Laboratory, Aiken SC (2015).

14. S. E. Kesson, "The Immobilization of Cesium in SYNROC Hollandite," *Radioactive Waste Manag. Environ. Restor.*, **4** [1] pp. 53-72, (1983).